
BIARCHETYPE ANALYSIS: SIMULTANEOUS LEARNING OF OBSERVATIONS AND FEATURES BASED ON EXTREMES

A PREPRINT

Aleix Alcacer
Department of Mathematics
Jaume I University
aalcacer@uji.es

Irene Epifanio
Department of Mathematics
Jaume I University
epifanio@uji.es

Ximo Gual-Arnau
Department of Mathematics
Jaume I University

ABSTRACT

A new exploratory technique called biarchetype analysis is defined. We extend archetype analysis to find the archetypes of both observations and features simultaneously. The idea of this new unsupervised machine learning tool is to represent observations and features by instances of pure types (biarchetypes) that can be easily interpreted as they are mixtures of observations and features. Furthermore, the observations and features are expressed as mixtures of the biarchetypes, which also helps understand the structure of the data. We propose an algorithm to solve biarchetype analysis. We show that biarchetype analysis offers advantages over biclustering, especially in terms of interpretability. This is because biarchetypes are extreme instances as opposed to the centroids returned by biclustering, which favors human understanding. Biarchetype analysis is applied to several machine learning problems to illustrate its usefulness. The source code and examples both in R and Python are available at <https://github.com/aleixalcacer/JA-BIAA>.

Keywords Archetype analysis, biclustering, prototype, unsupervised learning.

1 Introduction

Cluster analysis (CLA) is one of the most widely used tools in exploratory data analysis. The idea of clustering is to make groups of observations in such a way that each group contains similar observations that are different to those of the rest of the groups. If the data consist of well-separated clusters, appropriate clustering techniques can obtain, on the one hand, the representative of each cluster (the mean or centroid of the cluster for the popular k -means technique), and, on the other hand, the assignments of each observation to one cluster, or a degree of belonging to each cluster for fuzzy clustering techniques.

However, CLA is also used as a segmentation technique in the absence of well-separated (clearly differentiated) clusters in data. Many times, data follow a fan-spread pattern, i.e. features vary continuously across observations. The centroids are located in the middle of the data cloud since data points have to be covered in such a way that the distance between them and the assigned centroid is minimized (see [Wu et al., 2016] about the relationship between CLA and set partitioning). In those cases, where data can be viewed as a superposition of various populations, it is of particular interest to use Archetype Analysis (AA) for segmenting [Keller et al., 2019].

Instead of segmenting on the centroids, AA segments on the extremes. AA was defined by [Cutler and Breiman, 1994]. The objective of AA is to represent the observations by means of a convex combination of archetypes, which in turn are convex combinations of observations. Archetypes or ‘pure types’ lie on the boundary of the convex hull of the data and are therefore extreme profiles. Being extreme instances rather than central instances makes human understanding and interpretation of data easier [Thureau et al., 2012] since human cognition prefers extreme opposites [Davis and Love, 2010]. An illustrative example of this was analyzed in [Cabero and Epifanio, 2020], where CLA and AA were compared and archetypes were much more informative and understandable than centroids, because archetypes are further apart from each other than centroids.

Biclustering is a data mining technique introduced by [Hartigan, 1972], although it was popularized by [Cheng and Church, 2000], who applied it to gene expression data analysis. In biclustering (also known as block clustering, co-clustering, or two-mode clustering), rows (observations) and columns (features) of a data matrix are simultaneously clustered. An excellent overview of biclustering and fuzzy biclustering is found in [Ferraro et al., 2021]. Biclustering is widely used in biological and medical applications [Zhao et al., 2012], especially in gene expression data [Kerr et al., 2008, Xie et al., 2019]. However, it is also applied in many other fields, such as marketing [Dolnicar et al., 2012], psychology [Van Mechelen et al., 2004], recommender systems [Forsati et al., 2013], sports [Kaiser, 2011, Shkedy et al., 2016], website traffic [Koutsonikola and Vakali, 2009], and many other pattern recognition applications, such as collaborative filtering, text mining, multimedia data processing and retrieval, etc. [Zhao et al., 2012, Henriques et al., 2015].

In recent years, there has been growing interest in AA. On the one hand, there has been an increasing number of papers proposing efficient computational methods to calculate AA [Mørup and Hansen, 2012, Chen et al., 2014, Bauckhage et al., 2015, Mair et al., 2017], with applications in computer vision. On the other hand, AA has been applied in other very diverse fields, such as, climatology [Steinschneider and Lall, 2015, Su et al., 2017], ergonomics [Epifanio et al., 2013, Alcacer et al., 2020], genetics [Shoval et al., 2012, Thøgersen et al., 2013, Wang and Zhao, 2022], image processing [Zois et al., 2017, Sun et al., 2017a, Sun et al., 2017b, Cabero and Epifanio, 2019], machine learning problems [Mørup and Hansen, 2012, Ragozini and D’Esposito, 2015, Alcacer et al., 2021, Keller et al., 2021], market research [Porzio et al., 2008], multi-document summarization [Canhasi and Kononenko, 2014], nanotechnology [Fernandez and Barnard, 2015], neuroscience [Tsanousa et al., 2015, Hinrich et al., 2016], sports [Eugster, 2012, Vinué and Epifanio, 2017, Vinué and Epifanio, 2019] and sustainability [Thureau et al., 2012]. Finally, other papers have proposed extensions and new methodologies derived from AA with applications in a broad spectrum of fields: kernel AA [Mørup and Hansen, 2012], AA with missing data [Mørup and Hansen, 2012, Epifanio et al., 2020], robust AA [Eugster and Leisch, 2011, Moliner and Epifanio, 2019], interval archetypes [D’Esposito et al., 2012], archetypoid analysis (ADA) [Vinué et al., 2015], functional AA [Epifanio, 2016b], data-driven prototype identification [Ragozini et al., 2017], archetypal networks [Ragozini and D’Esposito, 2015], probabilistic AA [Seth and Eugster, 2016b], AA for nominal [Seth and Eugster, 2016a, Cabero and Epifanio, 2020] and ordinal observations [Fernández et al., 2021], directional AA [Olsen et al., 2022], AA for shapes [Epifanio et al., 2018], deep AA [Keller et al., 2021], and outlier detection [Millán-Roures et al., 2018, Vinué and Epifanio, 2020, Cabero et al., 2021]. Nevertheless, no previous work has developed archetypal analysis for both rows and columns simultaneously, which we refer to as biarchetype analysis (biAA), co-archetype analysis or two-mode archetype analysis.

[Xie et al., 2019] reviews biclustering in biological and biomedical fields. They point out the need to improve the interpretability of biclustering results, and they also highlight that possible overlapping homogeneous submatrices have to be identified. This clashes with the idea of CLA, whose origin was to find separate (not overlapping) groups, but it is in the line with the basis of AA. Moreover, biclustering of human gene expression data has been used to identify phenotype–genotype associations in studies of common or rare diseases. Note that archetypes themselves are phenotypes [Keller et al., 2021]; in fact, archetypes have been used also to explain the evolutionary development of biological systems [Tendler et al., 2015]. Therefore, putting all this together, it seems that biAA could be a reasonable alternative to biclustering in biology, as biAA could improve the interpretability of results. Nevertheless, the fields of application of biAA are not just restricted to biology; they would be the same as for biclustering, i.e. biAA can be applied to many pattern recognition problems.

Our contributions consist of defining biAA for the first time, proposing a computational method to calculate it, whose implementation is available in the R package `biaa` <https://github.com/aleixalcacer/biaa> and the Python package `archetypes` <https://github.com/aleixalcacer/archetypes>, showing how it works and the advantages of using archetypes (extremes) rather than the centroids of biclustering in an illustrative example, and finally, applying it to several real data sets in different fields to demonstrate the usefulness of biAA in various problems.

The outline of the paper is as follows: previous methodologies (CLA, biclustering, fuzzy biclustering, AA) are reviewed in a common framework in Sec. 2. In Sec. 3, biAA is defined and a computational procedure is proposed. An illustrative example is used to exemplify biAA and compare it to biclustering. In Sec. 4, our proposal is applied to three real data sets. Some conclusions and ideas for future work are provided in Sec. 5.

2 Background

Matrix factorization is our common framework for describing the established methods (as used in [Maurizio, 2001] for clustering) and our proposal. Let $\mathbf{X}_{n \times m}$ be a data matrix with n observations and m continuous features (they should

be standardized in order to avoid problems if they measure different dimensions). Let $\alpha_{n \times k}$ and $\gamma_{c \times m}$ be matrices with values in $[0, 1]$. α is the membership matrix of the observations, while γ is the membership matrix of the features. \mathbf{Z} is the matrix of representative instances that approximates \mathbf{X} . The objective is to minimize: $\|\mathbf{X} - \alpha\mathbf{Z}\gamma\|^2$, with different constraints, where $\|\cdot\|$ stands for the Frobenius norm.

2.1 Clustering

For clustering, \mathbf{Z} is the matrix of centroids, which is computed by $\mathbf{Z} = (\alpha'\alpha)^{-1}\alpha'\mathbf{X}\gamma'(\gamma\gamma')^{-1}$, where $'$ denotes transpose.

- *k*-means clustering: The constraints are: $\sum_{g=1}^k \alpha_{ig} = 1$ with $\alpha_{ig} \in \{0, 1\}$ for $i = 1, \dots, n$ and $\gamma = \mathbf{I}_{m \times m}$ is the identity matrix of order m . The matrix $\mathbf{Z}_{k \times m} = (\alpha'\alpha)^{-1}\alpha'\mathbf{X}$ has the centroids of each one of k groups that partition the data set.
- Fuzzy clustering: In soft clustering, each observation is assigned membership to each group. The restrictions are: $\sum_{g=1}^k \alpha_{ig} = 1$ with $\alpha_{ig} \geq 0$ for $i = 1, \dots, n$ and $\gamma = \mathbf{I}_{m \times m}$. Again, the matrix $\mathbf{Z}_{k \times m}$ has the centroids of each one of k groups.
- Biclustering: This is also called double *k*-means with hard partitions by [Maurizio, 2001], where algorithms to solve it are proposed. The constraints are: $\sum_{g=1}^k \alpha_{ig} = 1$ with $\alpha_{ig} \in \{0, 1\}$ for $i = 1, \dots, n$ and $\sum_{h=1}^c \gamma_{hj} = 1$ with $\gamma_{hj} \in \{0, 1\}$ for $j = 1, \dots, m$. Now, the dimension of \mathbf{Z} is $k \times c$, since there are k groups for observations and c groups of variables.
- Fuzzy biclustering: This is also called fuzzy double *k*-means by [Maurizio, 2001]. The constraints are now continuous: $\sum_{g=1}^k \alpha_{ig} = 1$ with $\alpha_{ig} \geq 0$ for $i = 1, \dots, n$ and $\sum_{h=1}^c \gamma_{hj} = 1$ with $\gamma_{hj} \geq 0$ for $j = 1, \dots, m$. [Ferraro et al., 2021] proposed several algorithms for solving fuzzy double *k*-means with continuous data, called FDkM and FDkMpF (Fuzzy Double *k*-Means with polynomial fuzzifiers), whose Matlab implementations are available in [Ferraro et al., 2021].

Besides the previous framework, there are some proposals of model-based biclustering. In that case, it is supposed that data are generated by a mixture distribution, as in [Govaert and Nadif, 2003], referred to as BMM (Block Mixture Model). Instead of memberships, it returns the final posterior probabilities for rows and columns, in addition to the mean and variance of each co-cluster. This is implemented in the R package blockcluster [Bhatia et al., 2017].

2.2 Archetype analysis

In AA, $\mathbf{Z}_{k \times m} = \beta_{k \times n}\mathbf{X}_{n \times m}$, where $\sum_{l=1}^n \beta_{gl} = 1$ with $\beta_{gl} \geq 0$ for $g = 1, \dots, k$, i.e. the archetypes are mixture of the data. The other restrictions are: $\sum_{g=1}^k \alpha_{ig} = 1$ with $\alpha_{ig} \geq 0$ for $i = 1, \dots, n$ and $\gamma = \mathbf{I}_{m \times m}$. Therefore, the objective function to minimize subject to the previous constraints is:

$$\begin{aligned} RSS &= \|\mathbf{X} - \alpha\mathbf{Z}\|^2 = \|\mathbf{X} - \alpha\beta\mathbf{X}\|^2 = \\ &= \sum_{i=1}^n \sum_{j=1}^m \left(x_{ij} - \sum_{g=1}^k \alpha_{ig} z_{gj} \right)^2 = \\ &= \sum_{i=1}^n \sum_{j=1}^m \left(x_{ij} - \sum_{g=1}^k \alpha_{ig} \left(\sum_{l=1}^n \beta_{gl} x_{lj} \right) \right)^2. \end{aligned} \tag{1}$$

The α coefficients determine how much each archetype contributes to the approximation of each observation, i.e. α_{ig} is the weight of the archetype g for the i -th observation. Archetypes are built as mixtures of observations weighted by β coefficients.

If $k = 1$, the archetype coincides with the mean, but with $k > 1$, the archetypes are located on the boundary of the convex hull of the data [Cutler and Breiman, 1994]. Archetypes are not necessarily nested, so different k s may reveal distinct structures of the data. Therefore, as happens in other unsupervised statistical learning procedures, the selection of the number k of prototypes has to be determined. If we have prior knowledge of the arrangement of the data, k can be selected based on this. Otherwise, we can use a simple but effective heuristic method, the elbow criterion, which has been used elsewhere [Cutler and Breiman, 1994, Eugster and Leisch, 2009]. The elbow criterion consists

of displaying the RSS for different k values and choosing the value k as the position where the elbow is located. This method is also used in clustering.

[Cutler and Breiman, 1994] proposed an alternating minimizing algorithm to find the matrices α and β that minimizes RSS. This consists of alternating between estimating the best α for given archetypes \mathbf{Z} , and the optimum archetypes \mathbf{Z} for given α . In each phase, convex least squares problems have to be solved. They used a penalized version of the non-negative least squares algorithm [Lawson and Hanson, 1974].

3 Biarchetype analysis

3.1 Definition

In biAA, biarchetypes are $\mathbf{Z}_{k \times c} = \beta_{k \times n} \mathbf{X}_{n \times m} \theta_{m \times c}$, where $\sum_{l=1}^n \beta_{gl} = 1$ with $\beta_{gl} \geq 0$ for $g = 1, \dots, k$ and $\sum_{r=1}^m \theta_{rh} = 1$ with $\theta_{rh} \geq 0$ for $h = 1, \dots, c$, i.e. the archetypes are mixture of the data points and variables. There are k archetypes for rows and c for columns. The other restrictions are: $\sum_{g=1}^k \alpha_{ig} = 1$ with $\alpha_{ig} \geq 0$ for $i = 1, \dots, n$ and $\sum_{h=1}^c \gamma_{hj} = 1$ with $\gamma_{hj} \geq 0$ for $j = 1, \dots, m$. Therefore, the objective function to minimize subject to the previous constraints is:

$$\begin{aligned} RSS &= \|\mathbf{X} - \alpha \mathbf{Z} \gamma\|^2 = \|\mathbf{X} - \alpha \beta \mathbf{X} \theta \gamma\|^2 = \\ &= \sum_{i=1}^n \sum_{j=1}^m \left(x_{ij} - \sum_{g=1}^k \sum_{h=1}^c \alpha_{ig} \beta_{gl} \theta_{rh} \gamma_{hj} \right)^2 = \\ &= \sum_{i=1}^n \sum_{j=1}^m \left(x_{ij} - \sum_{g=1}^k \sum_{h=1}^c \alpha_{ig} \left(\sum_{l=1}^n \sum_{r=1}^m \beta_{gl} x_{lr} \theta_{rh} \right) \gamma_{hj} \right)^2. \end{aligned} \quad (2)$$

As before, the α coefficients determine how much each archetype contributes to the approximation of each observation, i.e. α_{ig} is the weight of the archetype g for the i -th observation. Analogously, the γ coefficients determine how much each archetype contributes to the approximation of each variable, i.e. γ_{hj} is the weight of the archetype h for the j -th variable. Biarchetypes are built as mixtures of observations and variables weighted by β and θ coefficients, respectively.

3.1.1 Location of biarchetypes

In this section, we state some results that help in understanding the behavior of the row and column vectors of the biarchetype matrix $\mathbf{Z}_{k \times c}$.

Let $\mathbf{X}_{n \times m}$ be a data matrix with n observations and m continuous features. We denote by \mathbf{x}_i^d , $i = 1, \dots, n$ the row vectors of the matrix $\mathbf{X}_{n \times m}$ (in this case observations) and by \mathbf{x}_i^f , $i = 1, \dots, m$ the column vectors of the matrix $\mathbf{X}_{n \times m}$ (in this case features). This notation will be the same for all the matrices used.

The problem is to find a matrix $\mathbf{Z}_{k \times c}$ with $1 \leq k \leq n$, $1 \leq c \leq m$, which is expressed as $\mathbf{Z}_{k \times c} = \beta_{k \times n} \mathbf{X}_{n \times m} \theta_{m \times c}$ and the matrices $\alpha_{n \times k}$, $\mathbf{Z}_{k \times c}$ and $\gamma_{c \times m}$ minimize

$$RSS = \|\mathbf{X}_{n \times m} - \alpha_{n \times k} \mathbf{Z}_{k \times c} \gamma_{c \times m}\|^2.$$

Now we distinguish several cases depending on the values of k and c .

- Case I: $k = 1$ and $c = 1$. In this case, $\alpha_{n \times 1} = (1, \dots, 1)'$ and $\gamma_{1 \times m} = (1, \dots, 1)$; then, the real value $\mathbf{Z}_{1 \times 1}$ that minimizes RSS is the mean of all entries in matrix $\mathbf{X}_{n \times m}$, that is,

$$\mathbf{Z}_{1 \times 1} = \frac{1}{nm} \sum_{i=1}^n \sum_{j=1}^m x_{ij}.$$

- Case II: $k = n$ and $c = m$. In this case we consider $\alpha_{n \times n} = \mathbf{I}_{n \times n}$ and $\gamma_{m \times m} = \mathbf{I}_{m \times m}$. Then, by choosing $\mathbf{Z}_{n \times m} = \mathbf{X}_{n \times m}$ we obtain $RSS = 0$.

- Case III: $1 \leq k < n$ and $c = m$. We consider $\gamma_{m \times m} = \mathbf{I}_{m \times m}$ and $\theta_{m \times m} = \mathbf{I}_{m \times m}$, then, the problem now consists of minimizing

$$RSS = \|\mathbf{X}_{n \times m} - \alpha_{n \times k} \mathbf{Z}_{k \times m}\|^2,$$

which is a typical problem in AA and the location of the archetypes is explained in [Cutler and Breiman, 1994] and reviewed in Sec. 2.2.

- Case IV: $k = n$ and $1 \leq c < m$. This is the case of finding only the archetypes of features, i.e. we consider $\alpha = \mathbf{I}_{n \times n}$ and $\beta = \mathbf{I}_{n \times n}$. As the Frobenius norm of a matrix is the same as the Frobenius norm of its transpose, $\|\mathbf{X} - \mathbf{Z}\gamma\|^2 = \|\mathbf{X}' - \gamma' \mathbf{Z}'\|^2$, features can adopt the role of observations when \mathbf{X} is transposed. Then, the same reasoning as in the preceding case entails a problem of AA.
- Case V: $k = 1$ and $1 < c < m$. In this case $\alpha = \mathbf{I}_{n \times n}$ and the problem of minimizing

$$RSS = \|\mathbf{X}_{n \times m} - (1, \dots, 1)' (\mathbf{Z}_{1 \times c} \gamma_{c \times m})\|^2,$$

is satisfied if the mean value $\frac{1}{n} \sum_{i=1}^n \mathbf{x}_i^d = (\bar{x}_1^d, \dots, \bar{x}_m^d) = (\mathbf{Z}_{1 \times c} \gamma_{c \times m})$ where $\bar{x}_j^d = \frac{1}{n} \sum_{i=1}^n x_{ij}$. Note that each real number \bar{x}_i^d belongs to the convex hull of the components of the vector $\mathbf{Z}_{1 \times c}$.

- Case VI: $c = 1$ and $1 < k < n$. In this case RSS is minimized if $\frac{1}{m} \sum_{i=1}^m \mathbf{x}_i^f = (\bar{x}_1^f, \dots, \bar{x}_n^f) = (\mathbf{Z}_{k \times 1}' \alpha'_{n \times k})$ where $\bar{x}_i^f = \frac{1}{m} \sum_{j=1}^m x_{ij}$. Note that each real number \bar{x}_i^f belongs to the convex hull of the components of the vector $\mathbf{Z}_{k \times 1}$.
- Case VII: $1 < k < n$ and $1 < c < m$.
Let us call $\mathbf{V}_{n \times c} = \mathbf{X}_{n \times m} \theta_{m \times c}$; then, each \mathbf{v}_j^f ($j = 1, \dots, c$) belongs to the convex hull C_X^f of the data \mathbf{x}_i^f ($i = 1, \dots, m$). Moreover, since $\mathbf{Z}_{k \times c} = \beta_{k \times n} \mathbf{V}_{n \times c}$, each vector \mathbf{z}_j^d ($j = 1, \dots, k$) belongs to the convex hull C_V^d of the vectors \mathbf{v}_i^d ($i = 1, \dots, n$).

Proposition 1 *Having fixed the matrix $\theta_{m \times c}$, there is a matrix of biarchetypes $\mathbf{Z}_{k \times c}$ such that each row vector \mathbf{z}_j^d ($j = 1, \dots, k$) belongs to the boundary of the convex hull C_V^d .*

Now, let us call $\mathbf{Y}_{k \times m} = \beta_{k \times n} \mathbf{X}_{n \times m}$; then, each \mathbf{y}_j^d ($j = 1, \dots, k$) belongs to the convex hull C_X^d of the data \mathbf{x}_i^d ($i = 1, \dots, n$). Moreover, since $\mathbf{Z}_{k \times c} = \mathbf{Y}_{k \times m} \theta_{m \times c}$, each vector \mathbf{z}_j^f ($j = 1, \dots, c$) belongs to the convex hull C_Y^f of the vectors \mathbf{y}_i^f ($i = 1, \dots, m$).

Proposition 2 *Having fixed the matrix $\beta_{k \times n}$, there is a matrix of biarchetypes $\mathbf{Z}_{k \times c}$ such that each column vector \mathbf{z}_j^f ($j = 1, \dots, c$) belongs to the boundary of the convex hull C_Y^f .*

Proof of Propositions 1 and 2 is detailed in Appendix A.

Example 1 *This toy example illustrates the location of the biarchetypes for different values of k and c , for the following matrix*

$$\text{ing matrix } \begin{pmatrix} 1 & 2 & 3 & 4 & 5 \\ 6 & 7 & 8 & 9 & 10 \\ 11 & 12 & 13 & 14 & 15 \\ 16 & 17 & 18 & 19 & 20 \\ 21 & 22 & 23 & 24 & 25 \end{pmatrix}.$$

For $k = 1$ and $c = 1$, $\mathbf{z} = 13$ (mean of all entries of the matrix according to Case I). For $k = 1$ and $c = 2$, $\mathbf{z} = (11 \ 15)$; here $(\bar{x}_1^d, \dots, \bar{x}_5^d) = (11, 12, 13, 14, 15)$ and each real number \bar{x}_i^d belongs to the convex hull of the components of \mathbf{z} according to Case V. For $k = 2$ and $c = 1$, $\mathbf{z} = \begin{pmatrix} 3 \\ 23 \end{pmatrix}$ and, according to Case VI, each real number \bar{x}_i^f belongs to the convex hull of the components of the vector \mathbf{z} . For $k = 2$ and $c = 2$, $\mathbf{z} = \begin{pmatrix} 1 & 5 \\ 21 & 25 \end{pmatrix}$. For this last case, $RSS = 0$, and, according to Case VII, the vectors \mathbf{z}_j^d and \mathbf{z}_j^f , $j = 1, 2$ are located at the boundary of convex sets.

Example 2 In this example, we will generate the data from a multivariate random distribution.

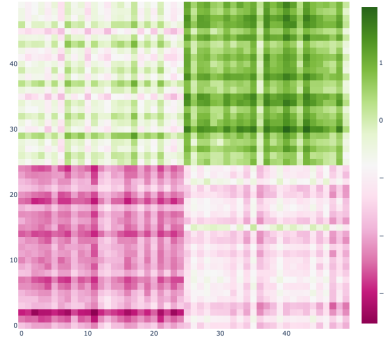
The covariance matrix for both rows and columns is:

$$\Sigma = \begin{pmatrix} 1 & 0.8 & \dots & 0.8 & 0.8 & 0 & 0 & \dots & 0 & 0 \\ 0.8 & 1 & \dots & 0.8 & 0.8 & 0 & 0 & \dots & 0 & 0 \\ \vdots & \vdots & \ddots & \vdots & \vdots & \vdots & \vdots & \ddots & \vdots & \vdots \\ 0.8 & 0.8 & \dots & 1 & 0.8 & 0 & 0 & \dots & 0 & 0 \\ 0.8 & 0.8 & \dots & 0.8 & 1 & 0 & 0 & \dots & 0 & 0 \\ 0 & 0 & \dots & 0 & 0 & 1 & 0.8 & \dots & 0.8 & 0.8 \\ 0 & 0 & \dots & 0 & 0 & 0.8 & 1 & \dots & 0.8 & 0.8 \\ \vdots & \vdots & \ddots & \vdots & \vdots & \vdots & \vdots & \ddots & \vdots & \vdots \\ 0 & 0 & \dots & 0 & 0 & 0.8 & 0.8 & \dots & 1 & 0.8 \\ 0 & 0 & \dots & 0 & 0 & 0.8 & 0.8 & \dots & 0.8 & 1 \end{pmatrix}$$

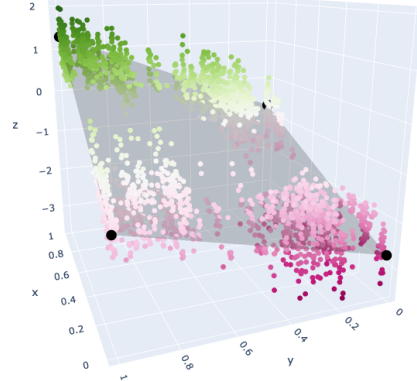
And the mean also for both rows and columns is:

$$\mu = (0 \dots 0)$$

The data generated can be seen in Figure 1a. and Figure 1b, the data are represented using the coefficients α and γ of biAA with $k = 2$ and $c = 2$. These coefficients are mapped to the x and y axes of the figure and the z axis represents the value of each observation. The biarchetypes are represented in black and, as seen, they are at the extremes of the data.



(a) Simulated data as a heatmap.



(b) Simulated data in the biarchetype space.

Figure 1: Representations of data and the biarchetypal space for Example 2, i.e. representation of the coefficients α and γ .

3.1.2 Selecting the number of biarchetypes

As in the case of AA, if there is no information available a priori, we can use the elbow criterion, but in this case, we look for the elbow of a surface instead of a curve. In biAA, we run biAA for different values of k and c and display their RSS values in a 3D plot. We select the point (k, c) where the surface "flattens", i.e. (k, c) is the point at which the RSS of the following points $(k + 1, c)$, $(k, c + 1)$, and $(k + 1, c + 1)$ stops decreasing drastically with respect to the RSS of the point (k, c) .

3.2 Algorithm

The following iterative method is proposed to solve biAA. It is based on alternating minimization as in the AA algorithm by [Cutler and Breiman, 1994].

1. Data preparation: To randomly initialize the matrices α , γ , β and θ , fulfilling the constraints in Sect. 3.1.
2. Repeat until RSS is sufficiently small or the number of maximum iterations is reached:

- (a) Find the best α (fixed γ): solve n convex least squares problems using $\mathbf{X}' = (\mathbf{Z}\gamma)' \alpha'$.
- (b) Find the best γ (fixed α): solve m convex least squares problems using $\mathbf{X} = (\alpha\mathbf{Z})\gamma$.
- (c) Recalculate the biarchetypes, where $^+$ stands for the Moore-Penrose pseudoinverse: $\mathbf{Z} = \alpha^+ \mathbf{X} \gamma^+$.
- (d) Find the best β (fixed θ): solve k convex least squares problems using $\mathbf{Z}' = (\mathbf{X}\theta)' \beta'$.
- (e) Find the best θ (fixed β): solve c convex least squares problems using $\mathbf{Z} = (\beta\mathbf{X})\theta$.
- (f) Recalculate the biarchetypes: $\mathbf{Z} = \beta\mathbf{X}\theta$.
- (g) Calculate the new RSS.

Note that the convex least squares problems can be solved as proposed by [Cutler and Breiman, 1994], i.e. using a penalized least squares problem [Lawson and Hanson, 1974]. The idea is, given a least squares problem $\mathbf{A}_{n \times k} \mathbf{X}_{k \times m} = \mathbf{B}_{n \times m}$, to add a row with constant elements C to \mathbf{A} and \mathbf{B} , in order to obtain a new problem $\mathbf{A}_{(n+1) \times k} \mathbf{X}_{k \times m} = \mathbf{B}_{(n+1) \times m}$, in such a way that RSS would be:

$$\begin{aligned}
 RSS &= \sum_{i=1}^{n+1} \sum_{j=1}^m \left(b_{ij} - \sum_{h=1}^k a_{ih} x_{hj} \right)^2 = \\
 &= \sum_{j=1}^m \left(\sum_{i=1}^n \left(b_{ij} - \sum_{h=1}^k a_{ih} x_{hj} \right)^2 + \left(b_{n+1,j} - \sum_{h=1}^k a_{n+1,h} x_{hj} \right)^2 \right) = \\
 &= \sum_{j=1}^m \left(\sum_{i=1}^n \left(b_{ij} - \sum_{h=1}^k a_{ih} x_{hj} \right)^2 + \sum_{j=1}^m \left(C - \sum_{h=1}^k C x_{hj} \right)^2 \right) = \\
 &= \sum_{j=1}^m \left(\sum_{i=1}^n \left(b_{ij} - \sum_{h=1}^k a_{ih} x_{hj} \right)^2 + \sum_{j=1}^m C^2 \left(1 - \sum_{h=1}^k x_{hj} \right)^2 \right).
 \end{aligned} \tag{3}$$

Therefore, if value C is high, the term $C^2 \left(1 - \sum_{h=1}^k x_{hj} \right)^2$ forces the convexity of the elements of \mathbf{X} in eq. 3.

3.3 Illustrative example and comparison with biclustering

The following example illustrates the use of biAA and its advantages in comparison with biclustering, especially when working with non-clustered data. We consider the data of 45 students from Universitat Jaume I, who reported the number of hours per week spent working on a subject at home over 17 weeks. The complete description of the data can be found in [Epifanio, 2016a]. Missing data are imputed by *mice* [van Buuren and Groothuis-Oudshoorn, 2011]. The data range from 0 to 10, with mean 4.94 and standard deviation 2.46. We apply biAA with $k = 4$ and $c = 3$, since the elbow is found at those values (see Fig. 2).

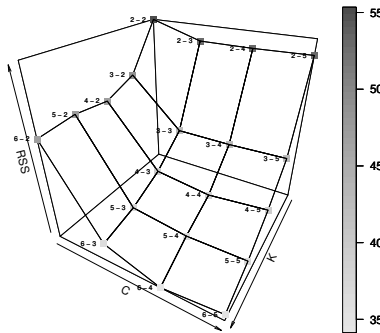


Figure 2: RSS for k from 2 to 6 and c from 2 to 5.

The γ coefficients for biAA, BMM, and FDkMpf are shown in Table 1 (we sort them in order to make the comments easier). FDkM was also applied, but the solution is not valid since the same prototypes are obtained for all the groups.

Table 1: The γ coefficients for biAA, BMM, and FDkMpf of the illustrative example.

1	0	0	1	0	0	1	0	0
0.71	0.12	0.17	1	0	0	1	0	0
0.57	0.42	0.01	1	0	0	0.85	0.08	0.08
0	0.80	0.20	0	0.01	0.99	0	0.5	0.5
0.13	0.76	0.11	0	1	0	0	0.5	0.5
0.14	0.86	0	0	1	0	0.29	0.35	0.35
0	0.80	0.20	0	1	0	0	0.5	0.5
0.01	0.99	0	0	0	1	0.2	0.4	0.4
0	0.90	0.11	0	1	0	0	0.5	0.5
0	0.89	0.11	0	1	0	0	0.5	0.5
0	0.42	0.58	0	1	0	0	0.5	0.5
0.05	0.45	0.5	0	0.96	0.04	0	0.5	0.5
0	0.62	0.38	0	1	0	0	0.5	0.5
0.05	0	0.95	0	0	1	0	0.5	0.5
0	0.04	0.96	0	0	1	0	0.5	0.5
0	0.10	0.91	0	0	1	0	0.5	0.5
0.13	0	0.87	0	0	1	0	0.5	0.5

(From now on, we will use archetype or archetypal instead of biarchetype or biarchetypal to simplify the language).

The feature similar to the first archetypal variable corresponds to the first week. The second and third weeks are also similar, but with a temporal gradation (0.71 and 0.57). Week 8, an intermediate week of the semester, is similar to the second archetypal variable. Other intermediate weeks (4, 5, 6, 7, 9, and 10) are also similar. Week 15, a week at the end of the semester, is similar to the third archetypal variable, as well as weeks 14, 16, and 17. Weeks 11, 12, and 13 are explained as mixtures (nearly 50% -50%) of the second and third archetypal variables. Note that the third week was also explained as a mixture close to 50% -50% of the first and second archetypal variables. In summary, the archetypal variables correspond to the profile of the beginning, middle and end of the semester, respectively. The weeks in the transitions between these temporal points are reflected as mixtures.

As regards the prototypical variables for biclustering methodologies, the first three weeks have probabilities of 1 (or nearly 1 for FDkMpf) for the first prototypical variable of BMM. Unlike biAA where gradation was found, the probabilities (memberships) are nearly crisp classifications for BMM, not only for the first prototypical variable, but for the rest as well. The intermediate weeks 5, 6, 7, 9, 10, 11, 12, and 13 have probabilities of 1 for the second prototypical variable, while the final weeks (14, 15, 16, and 17), and the intermediate weeks 4 and 8 have probabilities of nearly 1 or 1 for the third prototypical variable.

Note the difference with biAA. On the one hand, in BMM there is a lack of gradation over time in the memberships (no mixture is found, but the memberships are extremely high, nearly all ones), as if changes between adjoining weeks were radical (as breaking jumps) rather than smooth. Therefore, the information provided by biAA is richer. On the other hand, there are two intermediate weeks (4 and 8) belonging to the third prototypical variable corresponding to the end of semester weeks, which is not very coherent. Therefore, the information provided by biAA is more reasonable. Finally, the second and third prototypical variables are identical for FDkMpf, with 50%-50% or close degrees of membership for weeks 4 to 17. Therefore, the information returned by FDkMpf is poorer than that of BMM and biAA.

Table 2 displays the representative points \mathbf{Z} , archetypes or centroids for biAA and biclustering, respectively (we sort them in order to make the comments easier). The first archetype describes a student who works very few hours per week throughout the semester. The second archetype represents a student who studies very few hours throughout the semester, except at the end of the semester, when they work for 9 hours per week. The third archetype describes a student who works very few hours at the beginning of the semester (1h per week), many hours during the semester (10h per week), and intermediate hours (4h per week) at the end of the semester. The fourth archetype represents a student who studies many hours throughout the whole semester.

For BMM, the prototypes are not as pure as the archetypes. For example, there is no great difference between centroids 2 and 3: centroid 3 studies only one or one and a half hours more than centroid 2 per week. The centroids are not as intuitively interpretable as archetypes. Centroid 1 corresponds to a student who studies 2 or 3 hours throughout the semester; centroid 2 studies 2h per week at the beginning and 4 or 5h per week for the rest of the semester; centroid 3 works 4 hours at the beginning and 6 hours per week for the rest of the semester; while centroid 4 studies 5h per week at the beginning of the semester and 7 or 8 hours throughout the rest of the semester. It seems that centroids are

Table 2: The archetypes and centroids for biAA, BMM, and FDkMpf of the toy example.

1.54	2.36	0.36	1.67	2.07	3.49	2.03	3.28	3.28
1	2	9	2.32	4.15	5.02	2.74	4.89	4.89
1	10	4	3.79	5.70	6.05	3.42	5.97	5.97
8	6.32	9.36	5.01	7.69	6.60	5.55	6.97	6.97

limited to following a gradation according to the total number of hours studied throughout the semester rather than by differences in behavior throughout the semester. For FDkMpf, the comments are similar, but in addition there is no difference between the intermediate and final weeks. For example, the profiles of students 32 and 33, who are similar to archetype 2 (with α s of 0.84 and 0.88, respectively), would not be reflected by the centroids of BMM or FDkMpf. They belong to cluster 2 of BMM, with probabilities of 0.97 and 1, respectively. But this does not say anything about how far (or in which direction) from centroid 2 those students are. This happens because the goal of clustering is to assign the data to groups, not to explain the structure of the data more qualitatively.

4 Results and discussion

Like biclustering, biAA can be applied to a wide range of fields. In this section, we will apply it to biology, document analysis and community detection.

The code and data sets for reproducing the results including those in Sec. 3.3 are available at <https://github.com/aleixalcacer/JA-BIAA>.

4.1 Gene expression data

To show how biAA can be applied, we examine data from gene expression of cutaneous melanoma used in [Bittner et al., 2000, Rocci and Vichi, 2008]. Instead of meticulously re-analyzing this data set, we use it to highlight the salient features of biAA.

The aim of this study was to test the idea that molecular profiles generated by cDNA microarrays could be used to differentiate between several subtypes of cutaneous melanoma, a kind of skin cancer. mRNA was collected from the 31 cutaneous melanoma samples, and Cy5-labeled cDNA was created. All samples were examined with the same reference probe, identified as Cy3. For each sample, Cy5 and Cy3-labeled cDNA were combined and hybridized to a different melanoma microarray. Red and green lasers were used to scan the hybridization array, and the resulting image was then analyzed.

The same pre-processing was carried out as in [Bittner et al., 2000, Rocci and Vichi, 2008]. Only 3613 cDNAs of the 8150 observations were classified as well measured. Cy5/Cy3 expression ratios were computed for the accurately measured genes. Ratios that were more than or equal to 50 and less than or equal to 0.02 were reduced to 50 and 0.02, respectively. A logarithmic scale was applied to the derived ratios (base 2). The log ratios were adjusted so that the median log-ratio for each experiment was equal to zero by subtracting the median log-ratio within an experiment from all log-ratios for that experiment. Since a single reference probe was utilized in all experiments, there was no standardization between trials.

Using one minus the Pearson correlation coefficient of log-ratios as a measure of dissimilarity between two experiments, [Bittner et al., 2000] applied the average linkage hierarchical clustering on the 31 cutaneous melanoma samples and obtained two clusters of 12 and 19 samples.

Regarding [Rocci and Vichi, 2008], they used double k -means to analyze the same data set. In this case, the columns were centered and scaled to unit variance, finding that the separation between two columns is proportional to one minus the Pearson correlation coefficient. In particular, their analysis indicates that samples 4 and 7 are members of the ‘19-samples’ group obtained by [Bittner et al., 2000], i.e. the main cluster group. The membership of these two samples in [Rocci and Vichi, 2008] differs from that obtained by [Bittner et al., 2000].

In our case, we applied biarchetype analysis to the same data set as [Rocci and Vichi, 2008], extracting three archetypes for the genes (rows) and two archetypes for the melanoma samples (columns).

As can be seen in Fig. 3, regarding the melanoma samples, if we cluster the data using the location of the maximum archetypal coefficient γ (i.e. the archetype that is most similar to the sample), we obtain two clusters of 8 and 23 samples. Regarding the archetypes of the genes, the first two discriminate the two groups quite well, while the third archetype (or group of genes) is not expressed for any melanoma group.

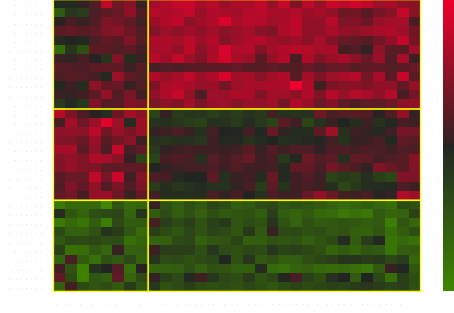


Figure 3: Representation of the most similar observations to each archetype. The color represents the expression ratio of each gene for each sample.



(a) Representation of the observations (α matrix) in their archetypal space. Each corner represents an archetype.

(b) Representation of the variables (γ matrix) in their archetypal space. Each corner represents an archetype.

Figure 4: Representations of the archetypal spaces for Gene expression data.

If we compare our results to those obtained by [Bittner et al., 2000], four samples are classified in different clusters. Samples 1, 4, 7 and 8 belong to the main cluster group with biAA (see Fig. 4), unlike results provided by [Bittner et al., 2000]. If we compare our results to those obtained by [Rocci and Vichi, 2008], two samples are classified in different clusters, samples 1 and 8. Classification group of samples 4 and 7 is shared with biAA and results by [Rocci and Vichi, 2008]. According to the γ coefficients of biAA, samples 4 and 7 are a nearly equal mixture between both archetypes, with the values of the coefficient being 0.4 and 0.6 corresponding to the first and second archetype for sample 4, and 0.45 and 0.55 corresponding to the first and second archetype for sample 7. Therefore, samples 4 and 7 could be in the border between both groups, which could explain the difference in classification by different methods. However, the γ coefficients for sample 8 and 1 are 0.75 (0.25) and 1 (0) for the second (first) archetype, respectively. In other words, sample 1 (and to lesser extent sample 8) should definitely be in the main group according with biAA.

4.2 Text documents

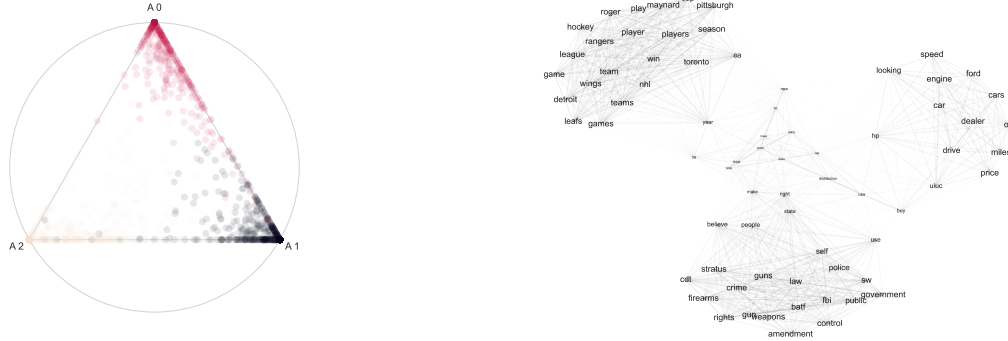
Another common use for biclustering is for clustering documents and words. In this case, we have applied biAA to a subset of the 20 Newsgroups collection, set up by [Lang, 1995]. Specifically, we have analyzed three topics: *rec.autos*, *rec.sport.hockey* and *talk.politics.guns*.

For each document, the number of times each word is repeated in the document has been stored in a count matrix, where each row represents a document, each column a word, and the values indicate how many times each word is repeated in each document.

In addition, a Tfidf transformer [Lang, 1995] was used to convert a count matrix into a normalized tf or tf-idf representation. Tf stands for term frequency, and tf-idf stands for term frequency multiplied by inverse document frequency. This is a standard term weighting method used in information retrieval, and it is also effective for classifying documents.

We have applied biarchetype analysis to this normalized matrix, obtaining three archetypal profiles for documents and three archetypal profiles for words.

In Fig. 5a, it is clear that the three archetypes discriminate the three groups of documents perfectly.



(a) Representation of the documents in their archetypal space (α values). The color represents the category of the document.

(b) Representation of the most similar words to each archetype (filtered using a threshold over the coefficient matrix). The weight of each edge is the cosine similarity between the two words in their archetypal space. This plot was created using the *networkx* Python package.

Figure 5: Results for the text documents example

Regarding the words, in Fig. 5b the words are represented as a graph. The weight of each edge represents the similarity of the words in terms of the archetypes (the gamma coefficients). The graph weights (i.e. the gamma coefficients) split the words into three groups, where the words within each group are related to one of the selected topics.

4.3 Community detection

Finally, we have also applied biAA to detect communities within the company Enron. For that, we have studied the data set described in [Klimt and Yang, 2004], which contains a collection of emails between the company’s employees.

We have created an adjacency matrix between employees, containing 1 if one employee has emailed another or 0 if the first one has never sent an email to the second one.

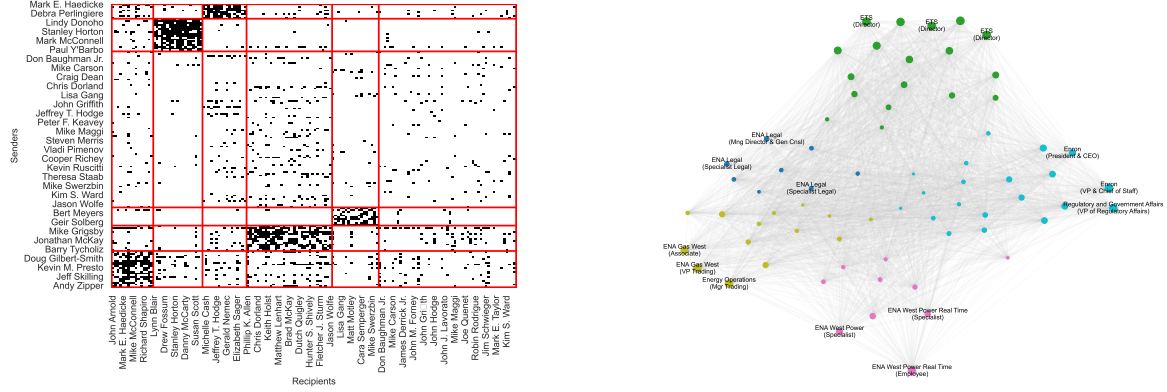
After applying biAA with $k = 6$ and $c = 6$ to this adjacency matrix, we obtained the results in Fig. 6a. In the ‘senders’ part, the group Z_3 could be omitted (represents employees who haven’t sent emails to a specific group). The same occurs with the group Z_6 in the ‘recipients’ part of the adjacency matrix.

If we analyze the employees from the point of view of who they send emails to, we obtain the results shown in Fig. 6b, in which we have removed Z_3 -like employees as they do not exchange emails with a specific group. As can be seen, the dark blue cluster represents the Legal department, the green one, the ETS department; the olive green one, the Gas/Energy department; the pink one, the West Power departments; and the blue one, Enron’s top management.

5 Conclusion

In this work, we have proposed a new unsupervised machine learning technique: biarchetype analysis. We have seen its usefulness in several problems in different fields. We have compared the results of biAA and biclustering in an illustrative example, showing not only the greater interpretability provided by biAA, but also the greater coherence of the results.

In this work, biAA has been defined for continuous data. In future work, it could be extended to other kinds of data, such as functional data, to which AA was also extended [Epifanio, 2016b]. Note that biclustering analysis of time series is used in many fields such as neuroscience [Castanho et al., 2022] and engineering [Silva et al., 2022]; therefore, biAA could also be used for the same problems. Biarchetypoid analysis could also be introduced in the same way that archetypoid analysis was defined [Vinué et al., 2015], where biarchetypes are not determined by mixtures of observations and features, but by concrete elements of the data set. Just as archetype analysis is sensitive to outliers, biAA is too. Robust biAA could be defined in the same way as robust AA was [Moliner and Epifanio, 2019]. Likewise, biAA for missing data could be defined as it was for AA [Epifanio et al., 2020], and it could be used in recommender



(a) The adjacency matrix ordered according to the archetypes obtained with BiAA.

(b) Representation of employees from the point of view of who they send emails to. The weight of each node is computed as in Fig. 5b. The size of each employee is proportional to how similar it is to its closest archetype and the color of each one is determined by the closest archetype.

Figure 6: Results for the community detection example

systems to find profiles of users and products, for instance. Another line of future work would be to apply biAA to different fields where biclustering analysis is applied, and to study more computational methods to calculate biAA, especially for big data. Finally, biAA could also be easily extended to high dimensions in a similar way to the decomposition proposed in [Tucker, 1966].

Acknowledgments

This research was partially supported by the Spanish Ministry of Universities (FPU grant FPU20/01825), Spanish Ministry of Science and Innovation (PID2020-118763GA-I00 and PID2020-115930GA-I00) and UJI-B2020-22 from Universitat Jaume I, Spain.

References

- [Alcacer et al., 2020] Alcacer, A., Epifanio, I., Ibáñez, M. V., Simó, A., and Ballester, A. (2020). A data-driven classification of 3D foot types by archetypal shapes based on landmarks. *PLOS ONE*, 15(1):e0228016.
- [Alcacer et al., 2021] Alcacer, A., Epifanio, I., Valero, J., and Ballester, A. (2021). Combining classification and user-based collaborative filtering for matching footwear size. *Mathematics*, 9(7).
- [Bauckhage et al., 2015] Bauckhage, C., Kersting, K., Hoppe, F., and Thureau, C. (2015). Archetypal analysis as an autoencoder. In *Workshop New Challenges in Neural Computation*, pages 8–15.
- [Bhatia et al., 2017] Bhatia, P. S., Iovleff, S., and Govaert, G. (2017). blockcluster: An R package for model-based co-clustering. *Journal of Statistical Software*, 76(9):1–24.
- [Bittner et al., 2000] Bittner, M., Meltzer, P., Chen, Y., Jiang, Y., Seftor, E., Hendrix, M., Radmacher, M., Simon, R., Yakhini, Z., Ben-Dor, A., et al. (2000). Molecular classification of cutaneous malignant melanoma by gene expression profiling. *Nature*, 406(6795):536–540.
- [Cabero and Epifanio, 2019] Cabero, I. and Epifanio, I. (2019). Archetypal analysis: an alternative to clustering for unsupervised texture segmentation. *Image Analysis & Stereology*, 38:151–160.
- [Cabero and Epifanio, 2020] Cabero, I. and Epifanio, I. (2020). Finding archetypal patterns for binary questionnaires. *SORT*, 44(1):39–66.
- [Cabero et al., 2021] Cabero, I., Epifanio, I., Piérola, A., and Ballester, A. (2021). Archetype analysis: A new subspace outlier detection approach. *Knowledge-Based Systems*, 217:106830.
- [Canhasi and Kononenko, 2014] Canhasi, E. and Kononenko, I. (2014). Weighted archetypal analysis of the multi-element graph for query-focused multi-document summarization. *Expert Systems with Applications*, 41(2):535 – 543.

- [Castanho et al., 2022] Castanho, E. N., Aidos, H., and Madeira, S. C. (2022). Biclustering fMRI time series: a comparative study. *BMC bioinformatics*, 23(1):1–30.
- [Chen et al., 2014] Chen, Y., Mairal, J., and Harchaoui, Z. (2014). Fast and Robust Archetypal Analysis for Representation Learning. In *CVPR 2014 - IEEE Conference on Computer Vision & Pattern Recognition*, pages 1478–1485.
- [Cheng and Church, 2000] Cheng, Y. and Church, G. M. (2000). Biclustering of expression data. In *Proceedings of the Eighth International Conference on Intelligent Systems for Molecular Biology*, volume 8, pages 93–103.
- [Cutler and Breiman, 1994] Cutler, A. and Breiman, L. (1994). Archetypal Analysis. *Technometrics*, 36(4):338–347.
- [Davis and Love, 2010] Davis, T. and Love, B. (2010). Memory for category information is idealized through contrast with competing options. *Psychological Science*, 21(2):234–242.
- [D’Esposito et al., 2012] D’Esposito, M. R., Palumbo, F., and Ragozini, G. (2012). Interval Archetypes: A New Tool for Interval Data Analysis. *Statistical Analysis and Data Mining*, 5(4):322–335.
- [Dolnicar et al., 2012] Dolnicar, S., Kaiser, S., Lazarevski, K., and Leisch, F. (2012). Biclustering: Overcoming data dimensionality problems in market segmentation. *Journal of Travel Research*, 51(1):41–49.
- [Epifanio, 2016a] Epifanio, I. (2016a). Cargas de trabajo no presencial ECTS arquetípicas del estudiantado: ¿cómo se reparten el trabajo semanalmente? In *Actas del Congreso Virtual: Avances en Tecnologías, Innovación y Desafíos de la Educación Superior ATIDES 2016*, pages 367–376.
- [Epifanio, 2016b] Epifanio, I. (2016b). Functional archetype and archetypoid analysis. *Computational Statistics & Data Analysis*, 104:24 – 34.
- [Epifanio et al., 2020] Epifanio, I., Ibáñez, M. V., and Simó, A. (2020). Archetypal analysis with missing data: see all samples by looking at a few based on extreme profiles. *The American Statistician*, 74(2):169–183.
- [Epifanio et al., 2018] Epifanio, I., Ibáñez, M. V., and Simó, A. (2018). Archetypal shapes based on landmarks and extension to handle missing data. *Advances in Data Analysis and Classification*, 12(3):705–735.
- [Epifanio et al., 2013] Epifanio, I., Vinué, G., and Alemany, S. (2013). Archetypal analysis: contributions for estimating boundary cases in multivariate accommodation problem. *Computers & Industrial Engineering*, 64(3):757–765.
- [Eugster and Leisch, 2009] Eugster, M. J. and Leisch, F. (2009). From Spider-Man to Hero - Archetypal Analysis in R. *Journal of Statistical Software*, 30(8):1–23.
- [Eugster, 2012] Eugster, M. J. A. (2012). Performance profiles based on archetypal athletes. *International Journal of Performance Analysis in Sport*, 12(1):166–187.
- [Eugster and Leisch, 2011] Eugster, M. J. A. and Leisch, F. (2011). Weighted and robust archetypal analysis. *Computational Statistics & Data Analysis*, 55(3):1215–1225.
- [Fernandez and Barnard, 2015] Fernandez, M. and Barnard, A. S. (2015). Identification of nanoparticle prototypes and archetypes. *ACS Nano*, 9(12):11980–11992.
- [Fernández et al., 2021] Fernández, D., Epifanio, I., and McMillan, L. F. (2021). Archetypal analysis for ordinal data. *Information Sciences*, 579:281–292.
- [Ferraro et al., 2021] Ferraro, M. B., Giordani, P., and Vichi, M. (2021). A class of two-mode clustering algorithms in a fuzzy setting. *Econometrics and Statistics*, 18:63–78.
- [Forsati et al., 2013] Forsati, R., Doustdar, H. M., Shamsfard, M., Keikha, A., and Meybodi, M. R. (2013). A fuzzy co-clustering approach for hybrid recommender systems. *International Journal of Hybrid Intelligent Systems*, 10(2):71–81.
- [Govaert and Nadif, 2003] Govaert, G. and Nadif, M. (2003). Clustering with block mixture models. *Pattern Recognition*, 36(2):463–473.
- [Hartigan, 1972] Hartigan, J. A. (1972). Direct clustering of a data matrix. *Journal of the American Statistical Association*, 67(337):123–129.
- [Henriques et al., 2015] Henriques, R., Antunes, C., and Madeira, S. C. (2015). A structured view on pattern mining-based biclustering. *Pattern Recognition*, 48(12):3941–3958.
- [Hinrich et al., 2016] Hinrich, J. L., Bardenfleth, S. E., Roge, R. E., Churchill, N. W., Madsen, K. H., and Mørup, M. (2016). Archetypal analysis for modeling multisubject fMRI data. *IEEE Journal on Selected Topics in Signal Processing*, 10(7):1160–1171.
- [Kaiser, 2011] Kaiser, S. (2011). *Biclustering: methods, software and application*. PhD thesis, Ludwig-Maximilians-Universität München.

- [Keller et al., 2021] Keller, S. M., Samarin, M., Arend Torres, F., Wieser, M., and Roth, V. (2021). Learning extremal representations with deep archetypal analysis. *International journal of computer vision*, 129(4):805–820.
- [Keller et al., 2019] Keller, S. M., Samarin, M., Wieser, M., and Roth, V. (2019). Deep archetypal analysis. In Fink, G. A., Frintrop, S., and Jiang, X., editors, *Pattern Recognition*, pages 171–185, Cham. Springer International Publishing.
- [Kerr et al., 2008] Kerr, G., Ruskin, H. J., Crane, M., and Doolan, P. (2008). Techniques for clustering gene expression data. *Computers in Biology and Medicine*, 38(3):283–293.
- [Klimt and Yang, 2004] Klimt, B. and Yang, Y. (2004). The Enron corpus: A new dataset for email classification research. In *Proceedings of the 15th European Conference on Machine Learning*, page 217–226, Berlin, Heidelberg. Springer-Verlag.
- [Koutsonikola and Vakali, 2009] Koutsonikola, V. A. and Vakali, A. (2009). A fuzzy bi-clustering approach to correlate web users and pages. *IJ Knowledge and Web Intelligence*, 1(1/2):3–23.
- [Lang, 1995] Lang, K. (1995). Newsweeder: Learning to filter netnews. In *Proceedings of the Twelfth International Conference on Machine Learning*, pages 331–339.
- [Lawson and Hanson, 1974] Lawson, C. L. and Hanson, R. J. (1974). *Solving Least Squares Problems*. Prentice Hall, Englewood Cliffs.
- [Mair et al., 2017] Mair, S., Boubekki, A., and Brefeld, U. (2017). Frame-based data factorizations. In *International Conference on Machine Learning*, pages 2305–2313.
- [Maurizio, 2001] Maurizio, V. (2001). Double k-means clustering for simultaneous classification of objects and variables. In Borra, S., Rocci, R., Vichi, M., and Schader, M., editors, *Advances in Classification and Data Analysis*, pages 43–52, Berlin, Heidelberg. Springer.
- [Millán-Roures et al., 2018] Millán-Roures, L., Epifanio, I., and Martínez, V. (2018). Detection of anomalies in water networks by functional data analysis. *Mathematical Problems in Engineering*, 2018(Article ID 5129735):13.
- [Moliner and Epifanio, 2019] Moliner, J. and Epifanio, I. (2019). Robust multivariate and functional archetypal analysis with application to financial time series analysis. *Physica A: Statistical Mechanics and its Applications*, 519:195 – 208.
- [Mørup and Hansen, 2012] Mørup, M. and Hansen, L. K. (2012). Archetypal analysis for machine learning and data mining. *Neurocomputing*, 80:54–63.
- [Olsen et al., 2022] Olsen, A. S., Høegh, R. M. T., Hinrich, J. L., Madsen, K. H., and Mørup, M. (2022). Combining electro- and magnetoencephalography data using directional archetypal analysis. *Frontiers in Neuroscience*, 16.
- [Porzio et al., 2008] Porzio, G. C., Ragozini, G., and Vistocco, D. (2008). On the use of archetypes as benchmarks. *Applied Stochastic Models in Business and Industry*, 24:419–437.
- [Ragozini and D’Esposito, 2015] Ragozini, G. and D’Esposito, M. R. (2015). Archetypal networks. In *Proceedings of the 2015 IEEE/ACM International Conference on Advances in Social Networks Analysis and Mining 2015*, pages 807–814, New York, NY, USA. ACM.
- [Ragozini et al., 2017] Ragozini, G., Palumbo, F., and D’Esposito, M. R. (2017). Archetypal analysis for data-driven prototype identification. *Statistical Analysis and Data Mining: The ASA Data Science Journal*, 10(1):6–20.
- [Rocci and Vichi, 2008] Rocci, R. and Vichi, M. (2008). Two-mode multi-partitioning. *Computational Statistics and Data Analysis*, 52:1984–2003.
- [Seth and Eugster, 2016a] Seth, S. and Eugster, M. J. A. (2016a). Archetypal analysis for nominal observations. *IEEE Trans. Pattern Anal. Mach. Intell.*, 38(5):849–861.
- [Seth and Eugster, 2016b] Seth, S. and Eugster, M. J. A. (2016b). Probabilistic archetypal analysis. *Machine Learning*, 102(1):85–113.
- [Shkedy et al., 2016] Shkedy, Z., Sengupta, R., and Perualila, N. J. (2016). Identification of local patterns in the NBA performance indicators. In *Applied Biclustering Methods for Big and High-Dimensional Data Using R*, pages 323–344. Chapman and Hall/CRC.
- [Shoval et al., 2012] Shoval, O., Sheftel, H., Shinar, G., Hart, Y., Ramote, O., Mayo, A., Dekel, E., Kavanagh, K., and Alon, U. (2012). Evolutionary trade-offs, Pareto optimality, and the geometry of phenotype space. *Science*, 336(6085):1157–1160.
- [Silva et al., 2022] Silva, M. G., Madeira, S. C., and Henriques, R. (2022). Water consumption pattern analysis using biclustering: When, why and how. *Water*, 14(12).

- [Steinschneider and Lall, 2015] Steinschneider, S. and Lall, U. (2015). Daily precipitation and tropical moisture exports across the Eastern United States: An application of archetypal analysis to identify spatiotemporal structure. *Journal of Climate*, 28(21):8585–8602.
- [Su et al., 2017] Su, Z., Hao, Z., Yuan, F., Chen, X., and Cao, Q. (2017). Spatiotemporal variability of extreme summer precipitation over the Yangtze river basin and the associations with climate patterns. *Water*, 9(11).
- [Sun et al., 2017a] Sun, W., Yang, G., Wu, K., Li, W., and Zhang, D. (2017a). Pure endmember extraction using robust kernel archetypoid analysis for hyperspectral imagery. *ISPRS Journal of Photogrammetry and Remote Sensing*, 131:147 – 159.
- [Sun et al., 2017b] Sun, W., Zhang, D., Xu, Y., Tian, L., Yang, G., and Li, W. (2017b). A probabilistic weighted archetypal analysis method with Earth mover’s distance for endmember extraction from hyperspectral imagery. *Remote Sensing*, 9(8):841.
- [Tendler et al., 2015] Tendler, A., Mayo, A., and Alon, U. (2015). Evolutionary tradeoffs, Pareto optimality and the morphology of ammonite shells. *BMC systems biology*, 9(1):1–12.
- [Thøgersen et al., 2013] Thøgersen, J. C., Mørup, M., Damkiær, S., Molin, S., and Jelsbak, L. (2013). Archetypal analysis of diverse *Pseudomonas aeruginosa* transcriptomes reveals adaptation in cystic fibrosis airways. *BMC Bioinformatics*, 14:279.
- [Thureau et al., 2012] Thureau, C., Kersting, K., Wahabzada, M., and Bauckhage, C. (2012). Descriptive matrix factorization for sustainability: Adopting the principle of opposites. *Data Mining and Knowledge Discovery*, 24(2):325–354.
- [Tsanousa et al., 2015] Tsanousa, A., Laskaris, N., and Angelis, L. (2015). A novel single-trial methodology for studying brain response variability based on archetypal analysis. *Expert Systems with Applications*, 42(22):8454 – 8462.
- [Tucker, 1966] Tucker, L. R. (1966). Some mathematical notes on three-mode factor analysis. *Psychometrika*, 31(3):279–311.
- [van Buuren and Groothuis-Oudshoorn, 2011] van Buuren, S. and Groothuis-Oudshoorn, K. (2011). mice: Multivariate imputation by chained equations in R. *Journal of Statistical Software*, 45(3):1–67.
- [Van Mechelen et al., 2004] Van Mechelen, I., Bock, H.-H., and De Boeck, P. (2004). Two-mode clustering methods: a structured overview. *Statistical Methods in Medical Research*, 13(5):363–394.
- [Vinué and Epifanio, 2017] Vinué, G. and Epifanio, I. (2017). Archetypoid analysis for sports analytics. *Data Mining and Knowledge Discovery*, 31(6):1643–1677.
- [Vinué and Epifanio, 2019] Vinué, G. and Epifanio, I. (2019). Forecasting basketball players’ performance using sparse functional data. *Statistical Analysis and Data Mining: The ASA Data Science Journal*, 12:534–547.
- [Vinué and Epifanio, 2020] Vinué, G. and Epifanio, I. (2020). Robust archetypoids for anomaly detection in big functional data. *Advances in Data Analysis and Classification*, pages 1–26.
- [Vinué et al., 2015] Vinué, G., Epifanio, I., and Alemany, S. (2015). Archetypoids: A new approach to define representative archetypal data. *Computational Statistics & Data Analysis*, 87:102 – 115.
- [Wang and Zhao, 2022] Wang, Y. and Zhao, H. (2022). Non-linear archetypal analysis of single-cell RNA-seq data by deep autoencoders. *PLoS computational biology*, 18(4):e1010025.
- [Wu et al., 2016] Wu, C., Kamar, E., and Horvitz, E. (2016). Clustering for set partitioning with a case study in ridesharing. In *IEEE 19th International Conference on Intelligent Transportation Systems (ITSC)*, pages 1384–1388.
- [Xie et al., 2019] Xie, J., Ma, A., Fennell, A., Ma, Q., and Zhao, J. (2019). It is time to apply biclustering: a comprehensive review of biclustering applications in biological and biomedical data. *Briefings in Bioinformatics*, 20(4):1450–1465.
- [Zhao et al., 2012] Zhao, H., Wee-Chung Liew, A., Z Wang, D., and Yan, H. (2012). Biclustering analysis for pattern discovery: current techniques, comparative studies and applications. *Current Bioinformatics*, 7(1):43–55.
- [Zois et al., 2017] Zois, E. N., Theodorakopoulos, I., and Economou, G. (2017). Offline handwritten signature modeling and verification based on archetypal analysis. In *2017 IEEE International Conference on Computer Vision (ICCV)*, pages 5515–5524.

A Proof of Propositions 1 and 2

Proof of *Proposition 1*.

Let us denote $\mathbf{H}_{n \times m} = \alpha_{n \times k} \mathbf{Z}_{k \times c} \gamma_{c \times m}$ and $\mathbf{R}_{n \times c} = \alpha_{n \times k} \mathbf{Z}_{k \times c}$; then, each \mathbf{r}_j^d ($j = 1, \dots, n$) belongs to the convex hull C_Z^d of \mathbf{z}_i^d ($i = 1, \dots, k$). Moreover, since $\mathbf{H}_{n \times m} = \mathbf{R}_{n \times c} \gamma_{c \times m}$, each vector \mathbf{h}_j^f ($j = 1, \dots, m$) belongs to the convex hull C_R^f of the vectors \mathbf{r}_i^f ($i = 1, \dots, c$).

Having fixed $\mathbf{Z}_{k \times c}$; that is, having fixed \mathbf{z}_j^d ($j = 1, \dots, k$), $RSS = \|\mathbf{X}_{n \times m} - \mathbf{H}_{n \times m}\|^2$ is minimized with respect to α 's and γ 's by choosing $\forall i = 1, \dots, n$, \mathbf{h}_i^d to be the point in the convex set defined by C_R^f and C_Z^d that is closest to \mathbf{x}_i^d .

Suppose without loss of generality that \mathbf{z}_1^d is strictly interior to C_V^d ; then choose t such that $\mathbf{z}(t) = \mathbf{z}_j^d + t(\mathbf{z}_1^d - \mathbf{z}_j^d)$ is on the boundary of C_V^d . Since the matrix $\theta_{m \times c}$ is considered fixed, the convex hull C of $\mathbf{z}(t), \mathbf{z}_2^d, \dots, \mathbf{z}_k^d$ contains the convex hull C_Z^d of $\mathbf{z}_1^d, \mathbf{z}_2^d, \dots, \mathbf{z}_k^d$; therefore, we obtain a larger set over which to minimize $RSS = \|\mathbf{X}_{n \times m} - \mathbf{H}_{n \times m}\|^2$.

Proof of *Proposition 2*.

Now, let us denote $\mathbf{S}_{k \times m} = \mathbf{Z}_{k \times c} \gamma_{c \times m}$; then, each \mathbf{s}_j^f ($j = 1, \dots, m$) belongs to the convex hull C_Z^f of \mathbf{z}_i^f ($i = 1, \dots, c$). Moreover, since $\mathbf{H}_{n \times m} = \alpha_{n \times k} \mathbf{S}_{k \times m}$, each vector \mathbf{h}_j^d ($j = 1, \dots, n$) belongs to the convex hull C_S^d of the vectors \mathbf{s}_i^d ($i = 1, \dots, k$).

As before, having fixed $\mathbf{Z}_{k \times c}$; that is, having fixed \mathbf{z}_j^d ($j = 1, \dots, k$), $RSS = \|\mathbf{X}_{n \times m} - \mathbf{H}_{n \times m}\|^2$ is minimized with respect to α 's and γ 's by choosing $\forall i = 1, \dots, n$, \mathbf{h}_i^f to be the point in the convex set defined by C_S^d and C_Z^f that is closest to \mathbf{x}_i^d .

Suppose without loss of generality that \mathbf{z}_1^f is strictly interior to C_Y^f ; then choose t such that $\mathbf{z}(t) = \mathbf{z}_j^f + t(\mathbf{z}_1^f - \mathbf{z}_j^f)$ is on the boundary of C_Y^f . Since the matrix $\beta_{k \times n}$ is considered fixed, the convex hull C of $\mathbf{z}(t), \mathbf{z}_2^f, \dots, \mathbf{z}_c^f$ contains the convex hull C_Y^f of $\mathbf{z}_1^f, \mathbf{z}_2^f, \dots, \mathbf{z}_c^f$; therefore we obtain a larger set over which to minimize $RSS = \|\mathbf{X}_{n \times m} - \mathbf{H}_{n \times m}\|^2$.